UNIVERSIDADE DE SÃO PAULO

INSTITUTO DE FÍSICA
CAIXA POSTAL 20516
01498 - SÃO PAULO - SP
BRASIL

PUBLICAÇÕES

IFUSP/P-908

GROUND-STATE CORRELATIONS AND TRANSVERSE ELECTRON SCATTERING

A. Mariano, E. Bauer and F. Krmpotić
Departamento de Física, Facultad de Ciencias Exactas,
Universidad Nacional de La Plata, 1900 La Plata, Argentina

A.F.R. de Toledo Piza
Instituto de Física, Universidade de São Paulo

Março/1991

PACS numbers: 21.30.+y, 21.65.+f, 25.30.Fj

GROUND-STATE CORRELATIONS AND TRANSVERSE ELECTRON SCATTERING

A. Mariano, E. Bauer and F. Krmpotić

Departamento de Física, Facultad de Ciencias Exactas,

Universidad Nacional de La Plata, 1900 La Plata, Argentina

A.F.R. de Toledo Piza

Instituto de Física, Universidade de São Paulo, CP 20516,

01498 São Paulo, Brasil

ABSTRACT

We reexamine the role of two particle-two hole (2p2h) ground state correlations (GSC) on electron scattering in the quasi-elastic region. An extended RPA including explicitly the interaction of 1p1h excitations with both 2p2h and 3p3h excitations in the final state is presented. Formulas for the longitudinal and transverse structure functions are given in the framework of the Fermi gas model of the nucleus. As an example, numerical results for the spin-isospin response in ^{56}Fe are shown. We conclude that the effect of the GSC on the static structure functions is negligible.

In quasielastic electron scattering the electron penetrates well inside the nucleus. It thus probes the bulk of the nuclear charge and magnetization densities, which are fairly well described by single-particle degrees of freedom of nucleons in nuclear matter. In other words, the detailed treatment of the electromagnetic structure function does not differ dramatically from the mean field result for nuclear matter.

In fact, the first systematic experimental results for the total inclusive (e,e') cross sections have been successfully described within the nuclear Fermi-gas model [1]. More recent experiments [2] have allowed for the separate determination of the longitudinal S_L and transverse S_T structure functions, related respectively to the charge and current density distributions of the nucleus. The observation that both S_L and S_T are poorly described by free structure functions came as a surprise, and gave rise to many attempts to understand the apparent failure of the independent particle picture. They range from conventional nonrelativistic many-body treatments, such as RPA, second RPA (SRPA) or extended second RPA (ESRPA) to relativistic mean field theories. Modifications of the nucleon properties inside the nuclear medium, as well as subnuclear degrees of freedom, generically called meson exchange currents (MEC) (such as Δ-excitations and π production), have also been considered.

The RPA correlations are important in the longitudinal structure function at low momentum transfer but become negligible at about 400-500 MeV/c. Regarding the transverse structure function, they produce the necessary quenching and lead to fitting the data fairly well in the low energy region, while at higher energies (and in particular in the dip-region between the quasi-elastic and the Δ-peak) the predicted value is too low as compared with experiment. This shortcoming points to the relevance

of more complicated processes.

The SRPA approximation is to a large extent a hybrid of the RPA and optical model approaches and takes into account the effect of the coupling of the 1p1h and 2p2h configurations in the final state [3,4]. This additional coupling redistributes the quasielastic strength over the q-ω plane; namely, it reduces the quasielastic peak heights broadening the distributions, shifts the position of the peaks, and enhances the high- and low-energy tails of both structure functions. The ESRPA incorporates also the 2p2h ground state correlations (GSC) in a pertubative way [5-7]. However, neither SRPA nor ESRPA are able to generate additional strength [6].

Two-body MEC, first considered in this context by Van Orden and Donnelly [8], can lead directly to two particle excitations in the continuum and two holes in the residual system. Also the one-body current operator, when combined to 2p2h GSC, produces the same final states. Both processes, as well as the corresponding interference terms, have been carefully studied by Alberico, Ericson and Molinari [9] in 1984. Since then it has been widely stated in the literature (e.g. refs. [10,11]) that these effects, and in particular the last one, considerably increases the transverse structure function in the dip-region, improving in this way agreement with data (see figs.9-12 in ref. [9]).

The chief purpose of the present letter is to bring into play the 3p3h excitations in the final state, which also become involved as soon as the 2p2h GSC are included. We will use the extended third RPA (ETRPA), of which the formalism developed in ref. [12] is

TDA limit. Most of the conclusions of the present work will be valid for both the longitudinal and the transverse structure functions. Therefore we sketch here the main formulas of the ETRPA in nuclear matter for both structure functions.

We start with the Bethe-Salpeter equation for the polarization propagator

$$G=G^0+G^0VG \; ; \; G^0(\omega)=\frac{1}{\Omega}\begin{bmatrix}[\hbar\omega-\mathcal{H}_0+i\eta]^{-1} & 0\\ 0 & -[\hbar\omega+\mathcal{H}_0-i\eta]^{-1}\end{bmatrix}, \qquad (1)$$

where $\mathcal{H}_0$ is the one-body Hamiltonian, V the residual interaction and $\Omega=3\pi^2A/2k_F^3$ the quantization volume. The upper and lower submatrices of the unperturbed polarization propagator G^0 are evaluated between forward np-nh and backward nh-np pairs, respectively, with n=1,2 and 3, and the response R is expressed in terms of G and the one-body operator $\mathcal{O}$. We get [13]

$$R = \mathbb{O}\cdot\mathbb{G}\mathbb{O} \; ; \; \mathbb{G} = \mathbb{G}^0 + \mathbb{G}^0\mathbb{V}\mathbb{G}, \qquad (2)$$

with

$$\mathbb{O} = \begin{bmatrix}\mathcal{O}_1\\ \mathcal{O}_2\\ \mathcal{O}_3\end{bmatrix} \; ; \; \mathbb{G}^0 = \begin{bmatrix}G^0_{11} & 0 & 0\\ 0 & G^0_{22} & 0\\ 0 & 0 & G^0_{33}\end{bmatrix} ; \qquad (3)$$

$$\mathbb{V} = \begin{bmatrix}V_{11} & V_{12} & V_{13}\\ V_{21} & V_{22} & V_{23}\\ V_{31} & V_{32} & V_{33}\end{bmatrix} \; ; \quad \mathbb{G} = \begin{bmatrix}G_{11} & G_{12} & G_{13}\\ G_{21} & G_{22} & G_{23}\\ G_{31} & G_{32} & G_{33}\end{bmatrix},$$

where $\mathcal{O}_n \equiv \langle n|\mathcal{O}|0\rangle$, $V_{nn'} \equiv \langle n|V|n'\rangle$, $G_{nn'} \equiv \langle n|G|n'\rangle$ and $G^0_{nn} \equiv \langle n|G^0|n\rangle$.

When V_{22}, V_{23}, V_{32} and V_{33} are neglected (as is usually done

[3-6,12]) the total polarization propagator can be put in the form:

$$\mathcal{G} = \begin{pmatrix} G_{11} & G_{11}V_{12}G^0_{22} & G_{11}V_{13}G^0_{33} \\ G^0_{22}V_{21}G_{11} & G^0_{22} & 0 \\ G^0_{33}V_{31}G_{11} & 0 & G^0_{33} \end{pmatrix}, \qquad (4)$$

where

$$G_{11} = \left[\left(G^0_{11}\right)^{-1} - V_{11} - \Sigma_{11}\right]^{-1}, \qquad (5)$$

and

$$\Sigma_{11} = V_{12}G^0_{22}V_{21} + V_{13}G^0_{33}V_{31}, \qquad (6)$$

is the particle-hole self-energy.

The primary focus of this work is to investigate the contribution of the terms $\mathcal{O}_2{\cdot}G^0_{22}\mathcal{O}_2$ and $\mathcal{O}_3{\cdot}G^0_{33}\mathcal{O}_3$ to the structure function

$$S(\vec{q},\omega) = \sum_{m>0} |\langle m|\mathcal{O}(\vec{q})|0\rangle|^2 \delta(\omega-\omega_m) = -\frac{\Omega}{\pi}\,\mathrm{Im}\,R(\vec{q},\omega), \qquad (7)$$

when one includes the GSC by first order perturbation theory, i.e.,

$$|0\rangle = |HF\rangle - (H^0)^{-1}V|HF\rangle. \qquad (8)$$

Thus we have to evaluate

$$S^{GSC} = -\frac{\Omega}{\pi}\mathrm{Im}(\mathcal{O}_2{\cdot}G^0_{22}\mathcal{O}_2 + \mathcal{O}_3{\cdot}G^0_{33}\mathcal{O}_3). \qquad (9)$$

For the sake of completeness, formulas for the zero order and RPA strength functions, S^0 and S^{RPA}, will also be shown.

The one body operators $\mathcal{O}$ carry the quantum numbers $I\equiv\{TSM\}$

which stand, respectively, for the isospin, the spin and the spin-projection on the quantazation axis chosen along the direction of the momentum transfer $\vec{q}$. They are of the form

$$\mathcal{O}^I(\vec{q}) \equiv \mathcal{O}^{I+}(-\vec{q}) = F_D(q)\frac{g^I}{2}\sum_{i=1}^{A} O^I_i(\vec{q})e^{-i\vec{q}\cdot\vec{r}_i}\ ;\ F_D(q) = \left[1+\left(\frac{qhc}{855MeV}\right)^2\right]^{-2}, \qquad (10)$$

where $F_D(q)$ is the usual electromagnetic γNN form factor [14]. When the convection current is neglected one has: $O^{000}=1$, $O^{100}_n=\tau_3(n)$ and $g^{000}=g^{100}=1$ for the electric operators and $O^{011}_n=i(\vec{q}\times\vec{\sigma}(n))$, $O^{111}_n=i(\vec{q}\times\vec{\sigma}(n))\tau_3(n)$ and $g^{011}=\mu_S\mu_0$, $g^{111}=\mu_V\mu_0$ (with $\mu_0=\hbar/2Mc$, $\mu_S=0.880$, $\mu_V=4.708$) for the magnetic operators. It is clear that the corresponding structure functions carry the same sets of quantum numbers, and that $R_L=R^{000}+R^{100}$ and $R_T=R^{011}+R^{111}$.

Expressed by means of dimensionless quantities $\vec{Q}=\vec{q}/k_F$ and $\nu=\hbar\omega/2\varepsilon_F$, the single particle structure functions read:

$$S^0(\vec{Q},\nu) = \mathcal{G}(Q)\frac{\Omega}{\varepsilon_F}\left(\frac{k_F}{2\pi}\right)^3 I(\vec{Q},\nu), \qquad (11)$$

with

$$\mathcal{G}_L(Q) = F_D(Q);\ \mathcal{G}_T(Q) = \left(\mu_S^2+\mu_V^2\right)\mu_0^2(Qk_F)^2F_D(Q), \qquad (12)$$

and

$$I(\vec{Q},\nu) = \int d\vec{X}\,\theta(|\vec{X}+\vec{Q}|-1)\,\theta(1-|\vec{X}|)\,\delta(\nu-\vec{X}\cdot\vec{Q}-Q^2/2). \qquad (13a)$$

We shall employ the so-called ring approximation, which neglects the exchange matrix elements of V. Moreover, we will deal

with an interaction of the form

$$V(q,\omega) = \sum_I w^I(q,\omega)\ \hat{O}^I(\hat{q})\cdot\hat{O}^I(\hat{q}) \ , \qquad (14)$$

where the operators $\hat{O}^I(\hat{q})$ are obtained from the operators $O^I(\vec{q})$ by the substitutions $\tau_3 \to \vec{\tau}$ and $\vec{q} \to \hat{q}$ and the dot represents the scalar product in both momentum-spin and isospin spaces.

The corresponding RPA strength functions are:

$$S_L^{RPA}(\vec{Q},\nu)=S_L^0(\vec{Q},\nu)\left\{\left[\left[1-v^{000}(Q,\nu)R(\vec{Q},\nu)\right]^2+\left[v^{000}(Q,\nu)I(\vec{Q},\nu)\right]^2\right]^{-1}\right. \qquad (15a)$$
$$\left.+\left[\left[1-v^{100}(Q,\nu)R(\vec{Q},\nu)\right]^2+\left[v^{100}(Q,\nu)I(\vec{Q},\nu)\right]^2\right]^{-1}\right\} ,$$

and

$$S_T^{RPA}(\vec{Q},\nu)=S_T^0(\vec{Q},\nu)\left\{\mu_S^2\left[\left[1-v^{011}(Q,\nu)R(\vec{Q},\nu)\right]^2+\left[v^{011}(Q,\nu)I(\vec{Q},\nu)\right]^2\right]^{-1}\right. \qquad (15b)$$
$$\left.+\mu_V^2\left[\left[1-v^{111}(Q,\nu)R(\vec{Q},\nu)\right]^2+\left[v^{111}(Q,\nu)I(\vec{Q},\nu)\right]^2\right]^{-1}\right\}\left(\mu_S^2+\mu_V^2\right)^{-1} ,$$

where

$$v^I(Q,\nu)=\frac{2}{\varepsilon_F}\left(\frac{k_F}{2\pi}\right)^3 w^I(Q,\nu) \ , \qquad (16)$$

and

$$R(\vec{Q},\nu)=-\frac{1}{\pi}\mathcal{P}\int d\vec{X}\,\theta(1-|\vec{X}|)\,\theta(|\vec{X}+\vec{Q}|-1)\left[\frac{2\vec{X}\cdot\vec{Q}+Q^2}{\nu^2-\left(\vec{X}\cdot\vec{Q}+Q^2/2\right)^2}\right] \ . \qquad (13b)$$

The first term in (9) (with 2p2h excitations on the energy

shell) give rise to six topologically distinct diagrams [9,15]. Two of them, labelled as 2P and 2H and which are the dominant ones, are displayed in the upper part of fig. 1; their analytic expressions are:

$$S_i^{CSC}(\vec{Q},\nu)=\frac{1}{4}\sum_{TSM}(2T+1)2^M\int d\vec{K}d\vec{L}\left[v^{TSM}(K,0)\right]^2\mathcal{S}_i(\vec{K},\vec{L},\vec{Q},\nu), \qquad (17)$$

with

$$\mathcal{S}_{2P}(\vec{K},\vec{L},\vec{Q},\nu)=\frac{\theta(|\vec{L}|-1)\theta(1-|\vec{K}+\vec{L}-\vec{Q}|)\theta(|\vec{L}-\vec{Q}|-1)}{[2\nu-2\vec{L}\cdot\vec{Q}+Q^2]^2} \qquad (18a)$$
$$\times S^0[K,\nu-\vec{L}\cdot(\vec{Q}-\vec{K})+(\vec{Q}-\vec{K})^2/2] \ ,$$

and

$$\mathcal{S}_{2H}(\vec{K},\vec{L},\vec{Q},\nu)=\frac{\theta(1-|\vec{L}|)\theta(|\vec{K}-\vec{L}-\vec{Q}|-1)\theta(1-|\vec{L}+\vec{Q}|)}{[2\nu-2\vec{L}\cdot\vec{Q}-Q^2]^2} \qquad (18b)$$
$$\times S^0[\vec{K},\nu-\vec{L}\cdot(\vec{Q}-\vec{K})-(\vec{Q}-\vec{K})^2/2] \ .$$

The second term in (9) (with 3p3h excitations on the energy shell) contains three linked diagrams, which are labeled as 3P, 3H and 3PH and are shown in the middle part of fig.1. The first two have the same topological structure as the graphs 2P and 2H with

$$\mathcal{S}_{3P}(\vec{K},\vec{L},\vec{Q},\nu)=-\frac{(|\vec{L}|-1)\theta(|\vec{K}-\vec{L}-\vec{Q}|-1)\theta(1-|\vec{L}+\vec{Q}|)}{[2\nu+2\vec{L}\cdot\vec{Q}-Q^2]^2} \qquad (18c)$$
$$\times S^0[\vec{K},\nu+\vec{L}\cdot(\vec{Q}+\vec{K})+(\vec{Q}+\vec{K})^2/2-K^2] \ ,$$

and

$$\mathcal{S}_{3H}(\vec{K},\vec{L},\vec{Q},\nu)=-\frac{\theta(1-|\vec{L}|)\theta(1-|\vec{K}+\vec{L}-\vec{Q}|)\theta(|\vec{L}-\vec{Q}|-1)}{[2\nu+2\vec{L}\cdot\vec{Q}+Q^2]^2}$$

$$\times S^0[\vec{K},\nu+\vec{L}\cdot(\vec{Q}+\vec{K})-(\vec{Q}+\vec{K})^2/2+K^2] \ . \qquad (18d)$$

It might be thought that the Pauli principle should prevent the diagram 3P and 3H from contributing. This is not correct, and the exclusion principle has to be ignored in the construction of 3p3h graphs. This fact is connected with the cancellation of the unlinked diagrams as explained in the lower part of the fig. 1.[1] The 3P term stems from the graph 3P' which involves the following events: i) two particles in levels h_1 and h_2 below the Fermi surface scatter into levels p_1 and p_2 above the Fermi surface (the spontaneous creation of 2p2h pairs from the unperturbed ground state) ; ii) the interaction with the electron next lifts the third particle in the state h, with $h_1 \neq h \neq h_2$, to the state p and then drops if again into the level h; iii) finally, the particles in the levels p_1 and p_2 scatter into the holes h_1 and h_2, leaving the electron to propagate freely. Now, the diagram 3P' can be rewritten as the sum of the diagrams 3P'' and 3P. The first one is unlinked and should be disregarded by Goldstone's theorem [17], leaving just the graph 3P.

1

The interpretation of the Pauli-violating diagrams 3P and 3H is analog to that of the graphs which represent the admixtures of the single particle excitation with 3p2h configurations [16].

While the terms 2P, 2H, 3P and 3H receive contributions from all v^I, only the residual interaction which carries the same quantum numbers TSM as the electromagnetic vertex O^I will contribute to the RPA-like diagram 3PH.

Numerical calculations have been performed with the following parametrization for the residual interaction within the spin-isospin channels:

$$v^{110}(q,\omega)=C_\pi(q,\omega)g'-C_\pi(q,\omega)\frac{q^2}{q^2+\mu_\pi^2}; v^{111}(q,\omega)=C_\pi(q,\omega)g'-C_\rho(q,\omega)\frac{q^2}{q^2+\mu_\rho^2}, \qquad (19)$$

where $g'=0.7$, $C_{\pi,\rho}(q,\omega)=\Gamma^2_{\pi,\rho}(q,\omega)f^2_{\pi,\rho}/\mu^2_{\pi,\rho}$, and

$$\Gamma_{\pi,\rho}(q,\omega)=\frac{\Lambda^2_{\pi,\rho}-(\mu_{\pi,\rho}c^2)^2}{\Lambda^2_{\pi,\rho}-(\hbar\omega)^2+(\hbar cq)^2} \ , \qquad (20)$$

with Λ_π=1.3 GeV and Λ_ρ=2 GeV [10]. Reliable momentum dependencies for the remaining coupling constants $v^I(q,\omega)$ are not available andtherefore will not be considered here. The contributions of each of the four diagrams mentioned above are shown in fig.2, together with sum of the first two and with the total sum. It is seen that the combined effect of the 2p2h and 3p3h excitations in the final state is very small. A similar result has been obtained recently in the study of the Gamow-Teller resonances [13].

Let us discuss now the static structure functions

$$S^{GSC}(Q)=\hbar\int S^{GSC}(Q,\nu)d\omega \ . \qquad (21)$$

The following relationships are fulfilled:

$$S^{GSC}_{2P}(Q) - S^{GSC}_{3H}(Q) = S^{GSC}_{2H}(Q) - S^{GSC}_{3P}(Q) = \mathcal{G}(Q) N_{>}/2 \ , \qquad (22)$$

where

$$N_{>} = \frac{\Omega}{2} \frac{k_F^3}{(2\pi)^3} \sum_{TSM} (2T+1) 2^M \int d\vec{K} d\vec{P}_1 d\vec{P}_2 \left[v^{TSM}(K,0) \right]^2 \times \frac{\theta(|\vec{P}_1|-1)\theta(1-|\vec{P}_1+\vec{K}|)\theta(|\vec{P}_2|-1)\theta(1-|\vec{P}_2-\vec{K}|)}{[K^2+\vec{K}\cdot(\vec{P}_1-\vec{P}_2)]^2} \ , \qquad (23)$$

and $N_{>}$ is the number of particles above the Fermi level [8]. Our calculation yields $N_{>}=16.2$, which means that about 29% of particles are excited from the ^{56}Fe core. Moreover, we get that $S^{GSC}_i(Q)/\mathcal{G}(Q) \simeq 7.7,\ 0.3,\ -8.0,\ -0.6$ and 0.1, for the diagrams 2P, 2H, 3P, 3H and 3PH, respectively. Thus the total strength which comes from the GSC is

$$S^{GSC}(Q) = S^{GSC}_{2P}(Q) + S^{GSC}_{2H}(Q) + S^{GSC}_{3P}(Q) + S^{GSC}_{3H}(Q) = 2[S^{GSC}_{2P}(Q) + S^{GSC}_{3P}(Q)] = 2[S^{GSC}_{2H}(Q) + S^{GSC}_{3H}(Q)] \simeq 0. \qquad (24)$$

The main conclusions regarding the GSC are as follows:

(1) The scattering processes 2P and 2H, introduced by Alberico, Ericson and Molinari [10] inflate the RPA strength by about 20% (33%) when the 2p2h states up to 200 MeV (500 MeV) are included.

(2) The ph-pair creation processes 3P and 3H, bring in here,

tend to cancel the above strength ending up much the same as it would have without any GSC at all.

It is worth mentioning that this result is rather insensitive to the residual interaction employed. We also stress that the above statements concern solely the value of the static structure functions, eq. (19). The actual energy distribution of the structure functions will depend furthermore on the combined effects of the strength redistributing contributions (self-energy effects and non-diagonal terms in the propagator $\mathcal{G}$). In particular, one may expect that the net effect of the latter will consist in shifting low energy strength upwards [4-8,14], thus still producing the effect of filling the dip between the quasi-elastic and Δ peaks. A detailed account of this will be reported elsewhere.

Acknowledgment

One of the authors (AFRTP) acknowledges support from the Argentine-ICTP Scientific Cooperation Program and from the Universidad Nacional de La Plata. He is also grateful for the warm hospitality extended to him while visiting this Institution. Three of us (AM, EB and FK) are fellows of the Consejo Nacional de Investigacines Cientificas y Técnicas, Argentina.

References

[1] R.R. Whitney et al., Phys. Rev. C 9 (1974) 2230.

[2] P.Barreau et al., Nucl.Phys. A 402 (1983) 515.

[3] G. Co', K.F. Quader, R.D. Smith and J. Wambach, Nucl. Phys. A 485 (1988) 61.

[4] S. Drozdz, M. Buballa, S. Krewald and J. Speth, Nucl. Phys. A501 (1989) 487.

[5] K. Takayanagi, K. Shimizu and A. Arima, Nucl. Phys. A 477 (1988) 205; Nucl. Phys. A 481 (1988) 313.

[6] S. Adachi and Lipparini, Nucl. Phys. A 489 (1988) 445.

[7] K. Takayanagi, Phys. Lett. B 230 (1989) 11; Phys. Lett. B 233 (1989) 271; Nucl. Phys. A 510 (1990) 162; Nucl. Phys. A 516 (1990) 276.

[8] J.W. Van Orden and T.W. Donnelly, Ann. Phys. (N.Y.) 131 (1981) 451.

[9] W.M. Alberico, M. Ericson and A. Molinari, Ann. Phys. (N.Y.) 154 (1984) 356.

[10] A. Hotta et al., Phys. Rev. C 30 (1984) 87; W.M. Alberico et al., Phys. Rev. C 34 (1986) 977.

[11] W.M. Alberico, R. Cenni and A. Molinari, Part. Nucl. Phys. 23 (1989) 171.

[12] A. Mariano, J. Hirsch and F. Krmpotić, Nucl. Phys. A 518 (1990) 523.

[13] P. Ring and P. Schuck, The nuclear many-body problem (Springer-Verlag, New York, 1980) p. 318.

[14] S. Fantoni and V.R. Padharipande, Nucl. Phys. A473 (1987) 234.

[15] W.M. Alberico, A. De Pace and A. Molinari, preprint DFTT 7/90.

[16] D.J. Thouless, Rep. Prog. Phys. 27 (1964) 53.

[17] J.Goldstone, Proc. Roy. Soc. (London), A 239 (1957) 267; A.L. Fetter and J.D. Walecka, Quantum theory of many-particle systems (Mc. Graw-Hill, New York, 1971) p. 111.

Figure Captions

Fig. 1- Diagrammatic representation of the second order spontaneous excitations from the unperturbed ground state. The upper row shows the most relevant processes with 2p2h states on the energy shell. The middle row illustrates the contributions to the structure function which come from the admixtures of 3p3h configurations in the final state. The lower part explains the origin of the Pauli-violating linked diagrams. The encircled crosses denote the one-body vertices and dots indicate the two-body matrix elements.

Fig. 2- Numerical results for the transverse structure function built on the GSC. The Fermi wave number is k_F=1.20 fm^{-1}. The individual contributions are indicated by dotted curves. The dot-dashed curve is the partial contribution of the 2P and 2H processes, while the continuous curve represent the total strength.

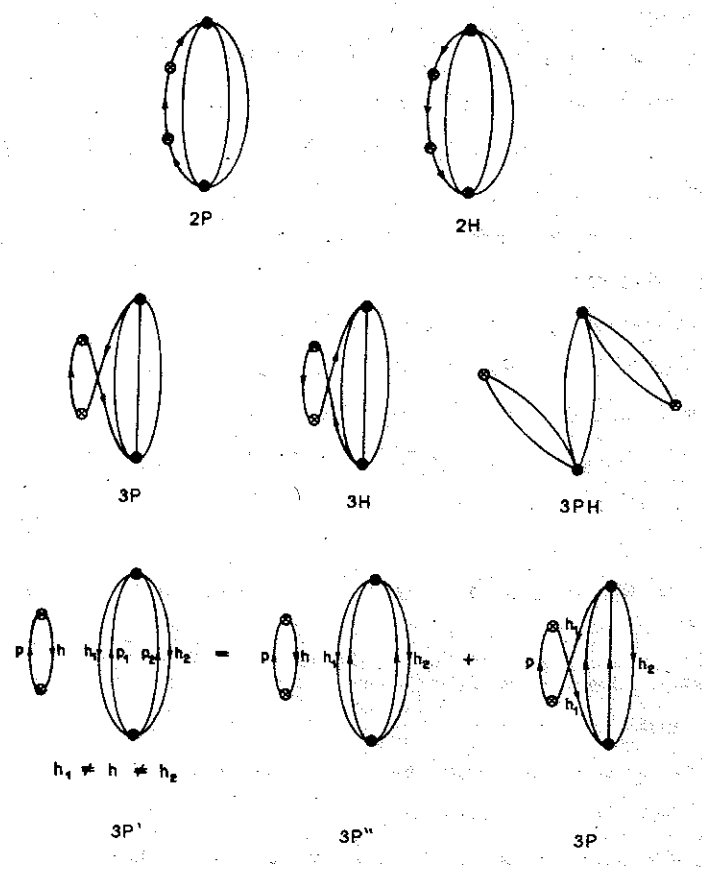

Fig 1

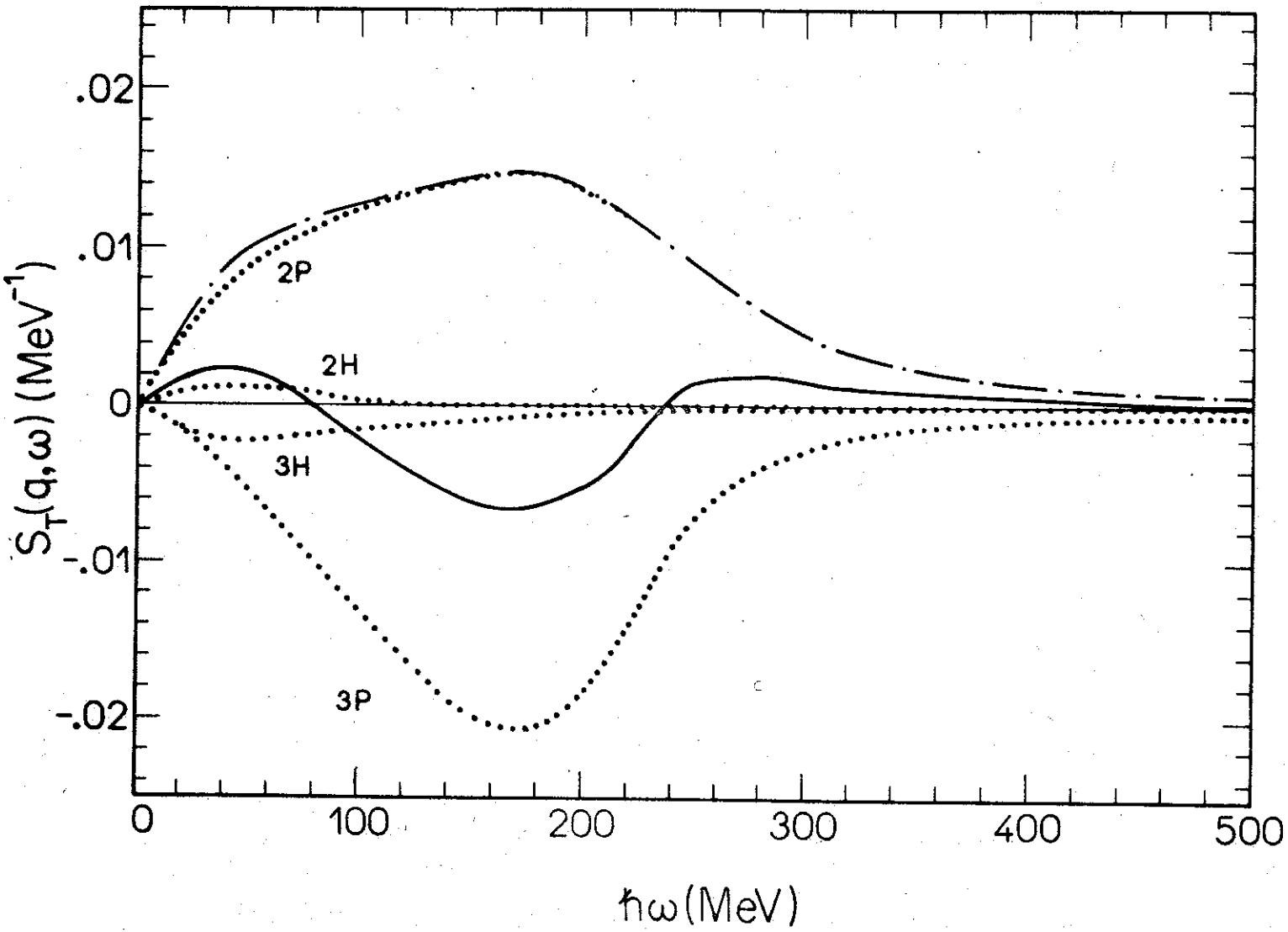
.02
.01
0
-.01
-.02
$S_T(q,\omega)$ (MeV^{-1})
2P
2H
3H
3P
0
100
200
300
400
500
$\hbar\omega$(MeV)

Fig 2